NeuroImage: Clinical 46 (2025) 103781

Contents lists available at ScienceDirect

NeuroImage: Clinical

journal homepage: www.elsevier.com/locate/ynicl

Functional and microstructural neurosubstrates between apathy and depressive symptoms in dementia

Sheng-Min Huang [a,b], Yen-Hsuan Hsu [c], Jir-Jei Yang [d], Chien-Yuan Lin [e], Min-Chien Tu [f,g,h,i,*], Li-Wei Kuo [b,j]

[a] Department of Pharmacology, College of Medicine, National Cheng Kung University, Tainan 701, Taiwan
[b] Institute of Biomedical Engineering and Nanomedicine, National Health Research Institutes, Miaoli 350, Taiwan
[c] Department of Psychology, National Chung Cheng University, Chiayi 621, Taiwan
[d] Department of Medical Imaging, Taichung Tzu Chi Hospital, Buddhist Tzu Chi Medical Foundation, Taichung 427, Taiwan
[e] GE Healthcare, Taipei 105, Taiwan
[f] Department of Neurology, Taichung Tzu Chi Hospital, Buddhist Tzu Chi Medical Foundation, Taichung 427, Taiwan
[g] Department of Neurology, School of Medicine, Tzu Chi University, Hualien 970, Taiwan
[h] Department of Neurology, China Medical University Hospital, Taichung 40447, Taiwan
[i] School of Medicine, College of Medicine, China Medical University, Taichung 40402, Taiwan
[j] Institute of Medical Device and Imaging, National Taiwan University College of Medicine, Taipei 100, Taiwan

ARTICLE INFO

Keywords:
Apathy Evaluation Scale
Beck's Depression Inventory
Resting-state functional MRI
Diffusion kurtosis imaging
Dementia

ABSTRACT

The overlapping features of depressive symptoms and apathy hinder their differentiation in clinical practice, and hence a greater understanding of their neurosubstrates in dementia and its subtypes is necessary. Ninety-two dementia patients (Alzheimer's disease [AD, n = 52]; subcortical ischemic vascular disease [SIVD, n = 40]), and 30 cognitively normal subjects were evaluated using the Apathy Evaluation Scale (AES), Beck's Depression Inventory (BDI), and brain magnetic resonance imaging (MRI). Grouped by AES/BDI scores, and hubs of depression/apathy were identified by comparing MRI metrics including fractional amplitude of low-frequency fluctuation (fALFF) of resting-state functional MRI, and mean kurtosis (MK) of diffusion kurtosis imaging. Associations between the hubs with depressive and apathy symptoms were analyzed. Comparing low-AES and high-AES groups, fALFF indicated pervasive changes mainly within the default mode network (DMN) and fronto-parietal network (FPN). Comparing low-BDI and high-BDI groups, fALFF reflected changes within the DMN, FPN, and salience network (SAN). Contrarily, MK showed focal changes within DMN and SAN regions from the same group-wise comparisons. While fALFF was more correlated with DMN/FPN for AES than BDI and more significantly correlated with SIVD than AD, MK was more correlated with the left anterior cingulate cortex and right insula for AES than BDI, but more significantly correlated with AD than SIVD (all $P < 0.01$). Topologically, the fALFF hubs for AES and BDI centered at the posterior and anterior poles, respectively. These findings suggest that dual-modal MRI could reflect the distinct neuropathological basis for apathy and depressive symptoms in AD and SIVD.

1. Introduction

Depressive symptoms and apathy are common neuropsychiatric symptoms in dementia patients (Miller, 2021; Cipriani, 2015). Depressive symptoms often manifest as a persistent feeling of sadness and loss of interest (Chand et al., 2023). Apathy is defined as "diminished motivation not attributable to diminished level of consciousness, cognitive impairment, or emotional distress" (Mann, 1990). Conceptually, depressive symptoms primarily stem from disordered mood, while apathy originates from impaired motivation and volition (Lanctôt, 2023). The early detection of depressive symptoms and apathy is essential, as they are both associated with negative impacts such as early institutionalization, functional dependence, and caregiver burden (Cipriani, 2015; Lanctôt, 2023). These two symptoms, however, can present with similar clinical features, such as reduced interest/initiative and diminished activity (Benoit, 2012). The overlapping features and

* Corresponding author at: Department of Neurology, China Medical University Hospital, No. 2, Yude Rd., North Dist., Taichung City 40447, Taiwan.
E-mail address: tmctmc30@yahoo.com.tw (M.-C. Tu).

https://doi.org/10.1016/j.nicl.2025.103781
Received 31 July 2024; Received in revised form 16 February 2025; Accepted 4 April 2025
Available online 6 April 2025

even the coexistence of depression and apathy (Benoit, 2012) often impede their prompt differentiation in clinical practice, hence hindering timely symptomatology-focused interventions. In some difficult cases, determining apathy or depressive symptoms could be highly observer-dependent. Empirically, the identification of depressive symptoms and apathy relies heavily on observations under a specific time frame of assessment, and the clinical features may assist clinicians in differentiating apathy from depression (Mortby, 2022). While some symptom-based questionnaires and scales are publicly available, it is inevitable for the observers to take both the environment (e.g., deprived environmental stimuli) and biological factors (e.g., impaired sensorium and/or cognition) into an overall account. As such, the underestimation on the severity of apathy and depressive symptoms remains to be an important issue in clinical practice. This is particularly challenging for people with dementia, in whom the occurrence of depressive symptoms and apathy mutually interact with their functional decline. Moreover, responses from cognitively impaired individuals can considerably bias geropsychiatric measures. A more objective rating approach, such as magnetic resonance imaging (MRI), can provide functional information and microstructural features via adequate imaging protocols. The usage of MRI is therefore a potential solution to characterize neurosubstrates relevant to depressive symptoms/apathy in people with dementia.

Brain atrophy, lacunes, and white matter changes are well-recognized common morphological changes observed in patients with depression/apathy (Wouts, 2020; Harris, 2022; Kempton, 2011). Despite diverse findings, anatomical hubs belonging to the frontal-limbic circuits and subcortical nucleus projections have recently attracted scientific attention (Kempton, 2011; Agüera-Ortiz, 2017; Zhuo, 2019). A *meta*-analysis reported volume reduction within multiple frontal regions, hippocampus, and basal ganglia in patients with major depressive disorder compared to healthy controls (Kempton, 2011). Another multimodal MRI study related white matter damage to apathy formation in patients with Alzheimer's disease (AD), particularly the corpus callosum and internal capsule (Agüera-Ortiz, 2017). The neurosubstrates relevant to depressive symptoms and apathy have been further explored in studies using diffusion tensor imaging (DTI) based on its preferable sensitivity in detecting microstructural changes within the white matter (Tu, 2017). In addition, diffusion kurtosis imaging (DKI), a recent diffusion MRI technique beyond DTI, has been proposed to improve the sensitivity of resolving complex tissue microstructures, and it has been shown to provide a higher classification rate of dementia subtypes (Tu, 2021).

The functional neurosubstrates for depressive symptoms and apathy have been discussed and hypothesized (Zhuo, 2019; Le Heron et al., 2018), while the neurocognitive frameworks remain to be validated. Resting-state functional MRI (rs-fMRI) monitors intrinsic brain network connectivity, and it has been used to study depressive symptoms and apathy, including regional rs-fMRI metrics (Yang, 2016), connectivity among hubs (Tumati, 2020; Wise, 2017), and integration of multiple rs-fMRI analyses (Altunkaya, 2022; Veer, 2010). Although these works have reported several potential hubs and interconnections associated with depressive symptoms or apathy, the relevant neurosubstrates remain to be confirmed, particularly due to the limited number of neuroimaging studies jointly evaluating depressive symptoms/apathy in the literature (Kim, 2011; Hollocks, 2015; Starkstein, 2009; Douven, 2017; Onoda and Yamaguchi, 2015; Dan, 2017). It is also unclear whether previous findings could be generalized to or vary across dementia subtypes (Tu, 2017; Altunkaya, 2022), and the intercorrelations of functional and microstructural neurosubstrates in depressive symptoms/apathy remain to be explored (Altunkaya, 2022).

AD and subcortical ischemic vascular disease (SIVD) contribute to a considerable portion of the dementia population (Guy and McKhann, 2011; Erkinjuntti, 2000). Although with different surrogate pathologies, these two dementia subtypes both exhibit slowly progressive courses that affect the features of apathy (Tu, 2017) and depression (Diniz, 2013). Together with the existence of mixed dementia (Jørgensen, 2020), exploring the neurosubstrates related to apathy and depression through a transdiagnostic approach can provide valuable information that assists early recognition of these psychological symptoms. Hence in the current research, we studied a prospective cohort who were evaluated for both depressive symptoms and apathy and underwent dual-modal brain MRI. We hypothesized that rs-fMRI and DKI metrics would be able to detect neurobiological changes of neuropsychiatric symptoms from functional and structural aspects. We aimed to (i) identify the functional and microstructural neuronal substrates related to depressive symptoms and apathy among dementia patients, and (ii) compare depressive symptom/apathy-related hubs according to the dementia subtype.

2. Materials and methods

2.1. Study design and participants

This prospective, observational, cross-sectional single-center study was approved by the Research Ethics Committee of the Hospital (#REC-107–28). Written informed consent was obtained from all participants. Following the same recruitment protocol (Tu, 2021), a total of 92 dementia patients (42 with SIVD (Erkinjuntti, 2000) and 50 with AD (Guy and McKhann, 2011) were recruited; patients with mixed dementia were excluded if the Hachinski Ischemic Scale was 5–6 (Hachinski, 1975). Another 30 older adults who were free from cognitive symptoms and had a Mini-Mental State Examination (MMSE) score $\geq$ 26 were recruited as the normal control (NC) group. All participants completed Beck's Depression Inventory (BDI) (Beck et al., 1996), Apathy Evaluation Scale-Clinician Version (AES) (Hsieh, 2012); global cognition evaluations (Clinical Dementia Rating, MMSE, and Cognitive Abilities Screening Instrument), neuropsychiatric inventory (NPI) (Fuh, 2001), and MRI scans. BDI, AES, and NPI of their validated Mandarin version were administered with a timing interval from MRI scan no longer than 3 weeks. To explore the shared and distinct hubs related to depressive symptoms and/or apathy, the dementia patients were initially dichotomized into two groups by the severity of depressive symptoms (i.e., low vs. high BDI; L-BDI vs. H-BDI; BDI median = 42 as the threshold) and apathy (low vs. high AES; L-AES vs. H-AES; AES median = 7 as the threshold). Between-group comparisons of both rs-fMRI and DKI metrics were made. We selected regions showing significant differences in" L-BDI vs. H-BDI" and "L-AES vs. H-AES" comparisons as the potential hubs for further analysis. The rationale for skipping the regions between "NC vs. any AES/BDI groupings" comparisons was to minimize the disease effect in the current transdiagnostic paradigm. Each hub with a significant change in rs-fMRI or DKI metric between dichotomized groups was then put into partial correlation analyses with BDI/AES among all participants, all dementia patients, and individual dementia subtypes (Fig. 1).

2.2. MRI acquisition

All participants underwent brain MRI on a 3 T MRI system (Discovery MR750, GE Medical Systems, Milwaukee, WI) with an eight-channel phased-array head coil. A spoiled gradient echo with RF-spoiling scheme (FSPRG) was employed for obtaining three-dimensional T1-weighted image (T1WI). The scanning parameters were repetition time (TR) of 7.904 ms, echo time (TE) of 3.06 ms, inversion time (TI) of 450 ms, flip angle of 12, field-of-view (FOV) of 240 mm, matrix size (MTX) of 240 × 240 × 160, achieving an isotropic voxel size of 1 mm^3. Gradient-echo echo-planar-imaging (EPI) was employed for resting-state fMRI scan. The scanning parameters were TR of 2500 ms, TE of 30 ms, flip angle of 90°, FOV of 200 mm, MTX of 64 × 64, 47 slices with slice thickness of 3 mm. A total of 154 consecutive volumes of EPI images were obtained. For diffusion kurtosis imaging (DKI), diffusion weighted spin-echo EPI sequence was used with 30 diffusion gradient directions and two b-vales (1000 and 2000 s/mm^2)

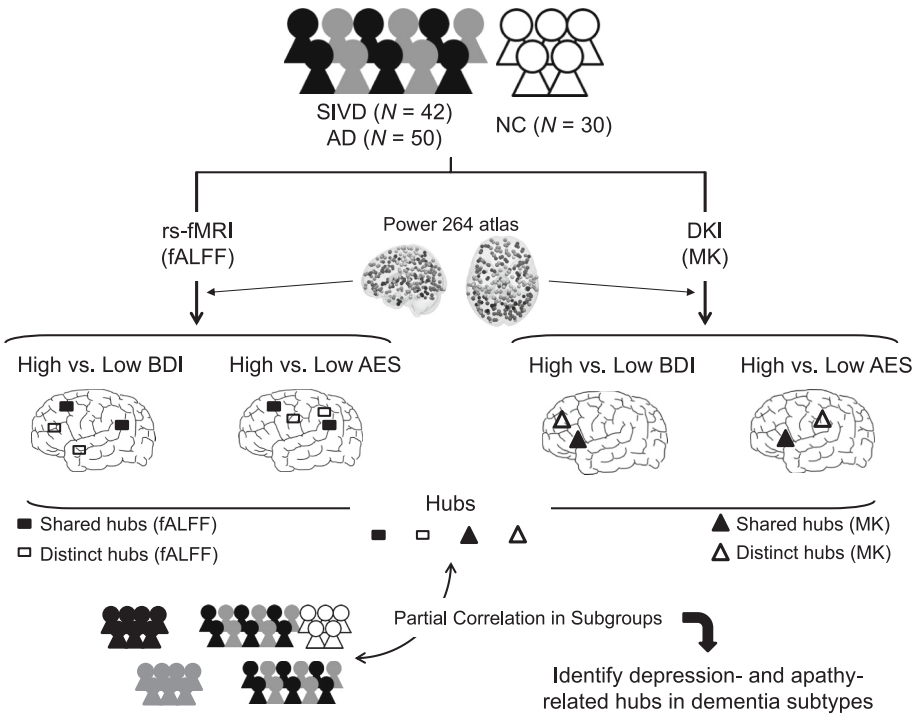

Fig. 1. Study workflow. The first stage of the current research primarily focused on identifying potential hubs related to depressive symptoms or apathy via dual-modal magnetic resonance imaging (MRI). Using the atlas defined by Power et al. (Power 264 atlas), regional values of fractional amplitude of low-frequency fluctuations (fALFF) and mean kurtosis (MK) were derived from resting-state functional MRI (rs-fMRI) and diffusion kurtosis imaging (DKI), respectively. The dementia patients were dichotomized by the Beck's Depression Inventory (BDI) levels (i.e., high versus low BDI) or the Apathy Evaluation Scale (AES) levels (i.e., high versus low AES) by their medians. Regions with significant between-group differences were identified: the identical regions by BDI and AES were termed shared hubs, and the different as distinct hubs. The second stage of the current research further explored the clinical relevance of these hubs using partial correlation among targeted subgroups to explore the aging and disease effects. SIVD, subcortical ischemic vascular disease; AD, Alzheimer's disease; NC, normal cognition.

along each diffusion gradient direction. With 5 un-weighted images (b0, b = 0 s/mm^2), a total of 65 volumes were acquired in each DKI dataset. Scanning parameters were TR of 6000 ms, TE of 68 ms, FOV of 240 mm, MTX of 96 × 96, 60 slices with slice thickness of 2.5 mm.

2.3. MRI processing

2.3.1. Resting-state fMRI (rs-fMRI)

For rs-fMRI dataset, image processing was performed by using the DPARSF toolbox (Yan and Zang, 2010). Preprocessing steps including removing first 10 time points, motion correction, slice timing, EPI to T1WI co-registration, spatial normalization to MNI space (ICBM512 template), and nuisance covariate regression (head motion, white matter, and CSF) were performed. The output data voxel size was set to 3 mm isotropic. Images with head motion exceeding half of the voxel width (1.5 mm) were excluded. The frequency range of 0.01 – 0.1 Hz was set for the calculation of voxel-wise fractional amplitude of low frequency fluctuations (fALFF).

2.3.2. Diffusion kurtosis imaging (DKI)

For DKI dataset, the image processing steps were the same to our previous work (Tu, 2021). All processing steps were carried out by using AFNI toolbox (https://afni.nimh.nih.gov) (Cox, 1996). Briefly, all T1WIs were aligned and normalized to standard MNI space, and all spatial warping transformation were applied on the DKI-derived metrics. After skull-stripping on the T1WI, an initial registration to MNI template was done via 12-parameter affine alignment. After that, tissue segmentation was performed on the roughly-aligned T1WI. The cerebral spinal fluid (CSF) voxels were set to zero to generate the CSF-free T1WI. The same CSF masking process was performed on the MNI template to generate the CSF-free MNI template. The consequent non-linear normalization consists of two steps: First, the CSF-free T1WI image was non-linearly co-registered to the CSF-free MNI template, and such non-linear warping transformation was then applied on the roughly-aligned T1WI to generate the first warped T1WI. Second, the first warped T1WI was then co-registered to the MNI template to generate the final normalized T1WI. Due to the different ventricular sizes across subjects, such two-step procedure was employed for adequate T1WI alignment outputs.

The alignment of DKI maps into MNI space was described as follows. First, the b0 images were linearly aligned to each subject's T1WI with 12-parameter affine transformation. Then the abovementioned linear and non-linear warp transformations for T1WI to MNI space were concatenated and applied onto the T1WI-aligned b0 image, resulting the b0 images in MNI space. The DKI maps were normalized to MNI space according to the warp transformation determined on b0 images. The DKI reconstruction was implemented using in-house MATLAB scripts (MathWorks, MA, USA). First, the diffusion weighted images (DWIs) underwent Gibbs ringing artifact removal by using MRtrix3 toolbox (Tournier, 2019), and were denoised with local PCA method (Manjón, 2013). DKI reconstruction was then performed according to the estimation approach of DKI model proposed by Tabesh *et al.* (Tabesh, 2011). The mean kurtosis (MK) was calculated in each subject's native space, and then aligned to MNI space according to the abovementioned steps. A ventricle mask was also generated from averaged b0 images of the SIVD group to avoid including unwanted ventricular voxels when calculating the regional DKI metrics.

2.4. MRI analysis

The dual-modal MRI metrics were analyzed among the brain regions defined by Power et al. (Power, 2011). Specifically, the regions from four standard resting-state networks, including the default mode network (DMN) (58 regions of interest [ROIs]), fronto-parietal network (FPN) (25 ROIs), salience network (SAN) (18 ROIs), and dorsal attention

network (DAN) (11 ROIs) were selected according to a hypothesis-driven paradigm (Altunkaya, 2022). The fractional amplitude of low-frequency fluctuation (fALFF) was utilized as the functional metric due to its standardized property (Zou, 2008). The mean kurtosis (MK) in the DKI model was used as the microstructural metric owing to its preferable performance in reflecting microstructural changes within the gray matter (Tu, 2021). To calculate the averaged MK and fALFF metrics within targeted regions, spherical regions with 10-mm diameter according to the center location defined by Power et al. were used.

In sum, the current research contains four steps: (i) hubs screening: four putative resting-state networks were analyzed, (ii) hubs selections: fALFF and MK datasets were contrasted by L-BDI vs. H-BDI and L-AES vs. H-AES comparisons, (iii) hubs characterization: the shared and distinct hubs between depression and apathy were reported, (iv) hubs identification: the clinical relevancy of the characterized hubs was determined by partial correlation analyses.

2.5. Statistical analysis

One-way analysis of variance and the chi-square test were used to compare demographic variables. Two-way analysis of variance was used to examine the interaction between AES/BDI groupings and dementia subtypes. Analysis of covariance (ANCOVA) was used to compare depressive/apathy indices and MRI metrics by controlling for age and education. The shared and distinct hubs of depression and apathy were contrasted separately by comparing fALFF or MK. Statistical significance was reported in conjunction with a partial eta-squared (ηp^2), with < 0.06/0.14/2 as the cut-off values for a small/medium/large effect (Lakens, 2013). As each ANCOVA conducted between groups by BDI and AES differs in case number pairs, we report effect size ηp^2 together with the *P* value of ANCOVA to provide clearer statistical information. In addition, the False Discovery Rate (FDR) was used to examine the results with considerations of multiple comparisons. Partial correlation analysis was used to determine the relationships between cerebral MRI metrics and depressive/apathy indices. To counterbalance the interactions between apathy and depressive symptoms, we reported the partial correlation results by controlling two sets of covariates. The first set of covariates included demographic and clinical parameters, including age, education, dementia subtype, and cognitive symptom duration. For the evaluation of depressive symptom correlates, AES was entered to be the second set of covariate. For the evaluation of apathy correlates, BDI was controlled. Considering potential interactions between AES and BDI, we additionally used linear regression analyses to examine the statistical power of the identified hubs. In this regression model, when the dependent variable was BDI, independent variables including (i) age, education, and cognitive symptom duration as the first tier, (ii) AES as the second tier, and (iii) hubs by the final partial correlation results (i.e., those showing significant after controlling demographics and AES) as the third tier were entered into each tier of regression analyses. The AES hubs were examined using a similar paradigm. These models were respecified on variance inflation factor greater than 5. All statistical tests were performed using SPSS version 25 (IBM, Armonk, NY). A *P* value < 0.01 was considered statistically significant.

3. Results

3.1. Demographics

Table 1 shows that the dementia patients grouped by BDI and AES were comparable in terms of age, education, sex, and dementia subtype, but varied in global cognitive scores. No significant interactions between dementia subtyping and BDI/AES groupings were noted (*P* = 0.113-0.914 from two way analysis of variance). The H-BDI and H-AES groups showed significantly worse global cognition than the L-BDI and L-AES groups (both *P* < 0.001). In addition, cognitive symptom duration differed significantly by AES but not BDI groupings. Age, education, and global cognition effects existed in the dementia groups compared to the NC group (all *P* < 0.001).

3.2. Depressive symptoms, apathy, and their associations

Table 2 shows comparisons of NPI-measured neuropsychiatric symptoms among the high and low BDI and AES groups. After controlling for age, education, cognitive symptom duration, and all global cognitive indices, the corresponding NPI subscores differed consistently in the dichotomized BDI groups or the dichotomized AES groups (L-BDI < H-BDI in depression; *P* = 0.003; NC/L-AES < H-AES in apathy; *P* ≤ 0.001). In addition, the H-BDI group showed significantly higher NPI total and appetite change scores than the L-BDI group (*P* = 0.003-0.005). The scatter plots also demonstrated that approximately 70 % of the dementia cases showed a coherence of depressive symptoms and apathy (i.e., patients classified in the H-BDI and H-AES groups, or *vice versa*) (Supplementary Data Fig. 1).

3.3. Shared and distinct hubs between depressive symptoms and apathy

The following MRI results were obtained after controlling for age and education.

3.3.1. fALFF dataset

Regarding rs-fMRI metrics, the H-BDI group showed significantly lower fALFF than the L-BDI group in the DMN (i.e., five ROIs within the left posterior cingulate cortex (PCC), left superior frontal gyrus (SFG) (two subregions), right superior temporal gyrus, and left middle temporal gyrus; *P* = 0.002-0.008), FPN (i.e., two ROIs within the left SFG and left middle frontal gyrus; *P* = 0.003-0.005), and SAN (i.e., two ROIs within the bilateral middle frontal gyrus; *P* = 0.003-0.007) (Supplementary Data Table 1). The H-AES group showed significantly

Table 1
Demographics of Participants.

	L-BDI (*N* = 49)	H-BDI (*N* = 43)	*F*/X^2¶	*P*	L-AES (*N* = 47)	H-AES (*N* = 45)	*F*/X^2¶	*P*	NC (*N* = 30)
Age (year-old)	76 ± 7.4	76 ± 7.1	6.740	0.002*	76 ± 7.5	76 ± 7.0	6.872	0.001*	71 ± 6.2
Education (years)	6 ± 4.6	5 ± 4.3	10.872	<.001*	5 ± 4.3	5 ± 4.7	10.005	<.001*	9 ± 4.1
Sex (Female/Male)	27/22	30/13	3.373	0.185	26/21	31/14	3.087	0.213	15/15
Dementia Subtype (SIVD/AD)	21/28	21/22	0.330	0.565-	21/26	21/24	0.003	0.848	–
Cognitive symptom duration (year)	2 ± 1.7	2 ± 2.2		0.114	2 ± 1.4	3 ± 2.3		0.007	–
Clinical Dementia Rating Sum of Box	3 ± 2.6	6 ± 3.5	34.417	<.001§	3 ± 1.7	7 ± 3.3	68.527	<.001§	0 ± 0.0
Mini-Mental State Exam	21 ± 4.6	18 ± 5.4	52.108	<.001§	22 ± 3.7	17 ± 5.3	74.766	<.001§	29 ± 1.0
Cognitive Abilities Screening Instrument	67 ± 14.0	55 ± 17.4	57.034	<.001§	69 ± 11.4	53 ± 17.2	75.652	<.001§	90 ± 4.5

L, low; H, high; BDI, Beck Depression Inventory; AES, Apathy Evaluation Scale; SIVD, subcortical ischemic vascular disease; AD, Alzheimer's disease; NC, normal Cognition. Data presented as Mean ± Standard deviation unless stated elsewhere. **¶:** Comparisons were made using the Analysis of variance (ANOVA) and Chi-square where appropriate. *P* values < 0.05 were marked in bold italics, with results from post-hoc Tukey analysis reported in the remark column. All participants were of right-handedness. * Significant differences between NC and patient groups. §: Significant differences across NC, low, and high groups either by BDI or AES.

Table 2
Neuropsychiatric Inventory of Participants.

	L-BDI ($N = 49$)	H-BDI ($N = 43$)	ANCOVA P	ANCOVA ηp^2	Post-Hoc Results	L-AES ($N = 47$)	H-AES ($N = 45$)	ANCOVA P	ANCOVA ηp^2	Post-Hoc Results	NC ($N = 30$)
Delusion	0 ± 0.6	1 ± 2.4	0.058	0.049		0 ± 0.6	1 ± 2.4	0.133	0.035		0 ± 0.0
Hallucination	9 ± 0.5	0 ± 1.2	0.902	0.002		0 ± 0.5	0 ± 1.2	0.365	0.018		0 ± 0.1
Agitation	0 ± 1.0	1 ± 1.9	0.368	0.018		0 ± 0.7	1 ± 1.9	0.805	0.004		0 ± 0.7
Depression	0 ± 1.0	2 ± 2.9	***0.004***	***0.093***	***L < H-BDI (P = 0.003)***	1 ± 1.3	2 ± 2.9	0.172	0.031		1 ± 2.0
Anxiety	0 ± 1.8	1 ± 1.9	0.379	0.017		1 ± 2.0	1 ± 1.6	0.075	0.045		1 ± 1.9
Euphoria	0 ± 0.1	0 ± 0.4	0.450	0.014		0 ± 0.1	0 ± 0.4	0.911	0.002		0 ± 0.0
Apathy	1 ± 2.2	3 ± 2.8	0.336	0.019		0 ± 0.6	4 ± 2.7	***0<.001***	***0.242***	***NC/L < H-AES (P ≤ 0.001)***	1 ± 1.4
Disinhibition	0 ± 1.2	1 ± 1.6	0.876	0.002		0 ± 0.1	1 ± 2.0	0.879	0.002		0 ± 0.1
Irritability	0 ± 0.6	1 ± 2.2	0.220	0.026		0 ± 0.5	1 ± 2.2	0.445	0.014		0 ± 1.2
Aberrant motor	0 ± 0.6	1 ± 1.3	0.302	0.021		0 ± 0.2	1 ± 1.4	0.308	0.021		0 ± 0.0
Sleep	1 ± 2.3	3 ± 2.8	0.404	0.016		1 ± 2.2	2 ± 2.9	0.832	0.003		2 ± 2.1
Appetite	0 ± 1.1	2 ± 2.8	***0.004***	***0.094***	***L < H-BDI (P = 0.003)***	1 ± 1.5	2 ± 2.6	0.246	0.025		1 ± 1.2
Total	6 ± 6.9	17 ± 13.8	***0.003***	***0.097***	***L < H-BDI (P = 0.005)***	5 ± 5.2	17 ± 14.0	0.084	0.043		6 ± 6.8

L, low; H, high; BDI, Beck Depression Inventory; AES, Apathy Evaluation Scale. Data presented as Mean ± Standard deviation. Comparisons are made by using the one-way analysis of covariance (ANCOVA) with age, education, cognitive symptom duration, Clinical Dementia Rating_sum of box, the Mini-Mental State Exam, and the Cognitive Abilities Screening Instrument as the covariates. The ANCOVA results were reported by a P value from the main effect, effect size, and P values from the post-hoc comparisons. Results with a P value < 0.01 were marked in bold italics. $0.01 \leq \eta p^2 < 0.06$ denotes a small effect, $0.06 \leq \eta p^2 < 0.14$ denotes a median effect, while $0.14 \leq \eta p^2$ denotes a large effect.

lower fALFF than the L-AES group in the DMN (i.e., five ROIs within the left middle temporal gyrus, left PCC, right precuneus, left SFG, and right middle frontal gyrus; $P = 0.001$-0.008), FPN (i.e., two ROIs within the bilateral precentral gyrus; $P \leq 0.001$-0.002), and DAN (i.e., one ROI within the left precuneus; $P = 0.003$) (Supplementary Data Table 2). The fALFF values within the DMN and FPN changed significantly according to BDI/AES grouping, with a greater effect size regarding apathy severity (as listed in Supplementary Data Table 1- 2). None of post-hoc results from fALFF dataset passed FDR correction, as the lowest P value remained slightly higher than the cut-offs (lowest P in BDI/AES = 0.000227/.00004; critical value = 0.00003).

3.3.2. MK dataset

Regarding DKI metrics, only two ROIs (the left anterior cingulate cortex (ACC) in the DMN and left SFG in SAN; both H-BDI < L-BDI; $P = 0.007$ −0.010) showed significant changes in H-BDI/L-BDI pairwise comparisons (Supplementary Data Table 3). Only two ROIs (the left ACC in the DMN and right insula in SAN; both H-AES < L-AES; $P = 0.001$ −0.008) showed significant changes in H-AES/L-AES pairwise comparisons (Supplementary Data Table 4). After FDR correction, some post-hoc results between NC and dementia remained significant ($P < 0.00040$, critical value = 0.00042), while none of post-hoc result between BDI/AES groupings among dementia patients passed the correction

3.3.3. Shared/distinct hubs between apathy and depressive symptoms

Fig. 2 summarizes the hubs contrasted by BDI/AES grouping (i.e., H-AES vs. L-AES and H-BDI vs. L-BDI). As $P < 0.01$ defined to be statistical significance, these reported significant results fall into median to large effect. In addition to the shared networks, BDI grouping showed distinct fALFF differences in the SAN, and AES grouping showed distinct fALFF differences in the DAN. Specifically, aside from the shared hubs (i.e., the left PCC and SFG), the hubs were distinct for depressive symptoms centered within the frontotemporal regions, while the hubs were distinct for apathy centered within the anterior and posterior poles. Regarding MK, the left ACC was the only shared hub between depressive symptoms and apathy. Distinct hubs were the left SFG for depressive symptoms and left insula for apathy. Both fALFF and MK showed hemispheric asymmetry, in which more hubs within the left hemisphere were identified.

Table 3
Correlations between the fALFF in the identified hubs and depressive symptom/apathy among dementia patients.

	Network	No.	Anatomical Region	SIVD + AD + NC ($N = 122$)	SIVD + AD ($N = 92$)	SIVD ($N = 42$)	AD ($N = 50$)
BDI	DMN	88 †	Lt Posterior Cingulate †	***−0.267*** **	***−0.360*** **	***−0.422*** **	−0.289
		100 †	Lt Superior Frontal Gyrus †	***−0.361*** *** §	***−0.335*** **	***−0.413*** **	−0.187
		103	Lt Superior Frontal Gyrus	−0.***263*****	−0.235	−0.262	−0.200
		128	Rt Superior Temporal Gyrus	−0.219	−0.233	−0.381	−0.082
		129	Lt Middle Temporal Gyrus	***−0.269*** **	***−0.295*** **	***−0.416*** **	−0.165
	FPN	178	Lt Superior Frontal Gyrus	***−0.318*** ***	***−0.352*** ***	−0.406	−0.274
		188	Lt Middle Frontal Gyrus	−0.205	***−0.278*** **	−0.378	−0.176
	SAN	205	Rt Middle Frontal Gyrus	−0.168	−0.209	−0.334	−0.041
		220	Lt Middle Frontal Gyrus	***−0.297*** **	***−0.336*** **	***−0.458*** **	−0.184
AES	DMN	74	Lt Middle Temporal Gyrus	−0.***265*****	−0.***305*****	−0.375	−0.220
		88 †	Lt Posterior Cingulate †	***−0.368***** ¶	***−0.393*** ***	−0.***450*****	−0.314
		89	Rt Precuneus	***−0.271*** **	−0.***297*****	−0.199	−0.336
		100 †	Lt Superior Frontal gyrus †	***−0.302*** ***	***−0.311*** **	−0.304	−0.286
		101	Rt Middle Frontal gyrus	***−0.278*** **	***−0.323*** **	−0.318	−0.312
	FPN	174	Lt Precentral Gyrus	***−0.300*** **	***−0.348*****	−0.384	−0.295
		187	Lt Precentral Gyrus	***−0.297*** ** ¶	−0.***324***** ¶	−0.245	−0.365
	DAN	260	Lt Precuneus	***−0.339*** *** ¶	***−0.351*** ***	−0.***420*****	−0.263

Partial correlation coefficients are reported after controlling for age, education, dementia subtype, cognitive symptom duration. ¶: Significant results on additional control for BDI. §: Significant results on additional control for AES. **/***: $P < 0.01/.001$. fALFF, fractional amplitude of low-frequency fluctuation; BDI, Beck's Depression Inventory; AES, Apathy Evaluation Scale; DMN, default mode network; FPN, frontoparietal network; SAN, salience network; DAN, dorsal attention network; SIVD, subcortical ischemic vascular disease; AD, Alzheimer's disease. †: Shared hubs between depressive symptoms and apathy. Number from the atlas by Power et al. (No.) is reported.

Table 4
Correlations between the MK in the identified hubs and depressive symptom/apathy among dementia patients.

	Network Label	No.	Anatomical Region	SIVD + AD + NC ($N = 122$)	SIVD + AD ($N = 92$)	SIVD ($N = 42$)	AD ($N = 50$)
BDI	DMN	109 †	Lt Anterior Cingulate Cortex †	***−0.305*** ***	***−0.331*** **	−0.282	***−0.392*** **
	SAN	214	Lt Superior Frontal Gyrus	−0.124	−0.252	−0.262	−0.238
AES	DMN	109 †	Lt Anterior Cingulate Cortex †	***−0.369*** *** ¶	***−0.379*** ***	−0.327	***−0.380*** **
	SAN	209	Rt Insula	***−0.352*** *** ¶	***−0.408*** *** ¶	***−0.408*** **	−0.366

Partial correlation coefficients are reported after controlling for age, education, dementia subtype, and cognitive symptom duration. ¶: Significant results on additional control for BDI. No significant results on additional control for AES. **/***: $P < 0.01/.001$. MK, mean kurtosis; BDI, Beck's Depression Inventory; AES, Apathy Evaluation Scale; DMN, default mode network; SAN, salience network; SIVD, subcortical ischemic vascular disease; AD, Alzheimer's disease. †: Shared hubs between depressive symptoms and apathy. Number from the atlas by Power et al. (No.) is reported.

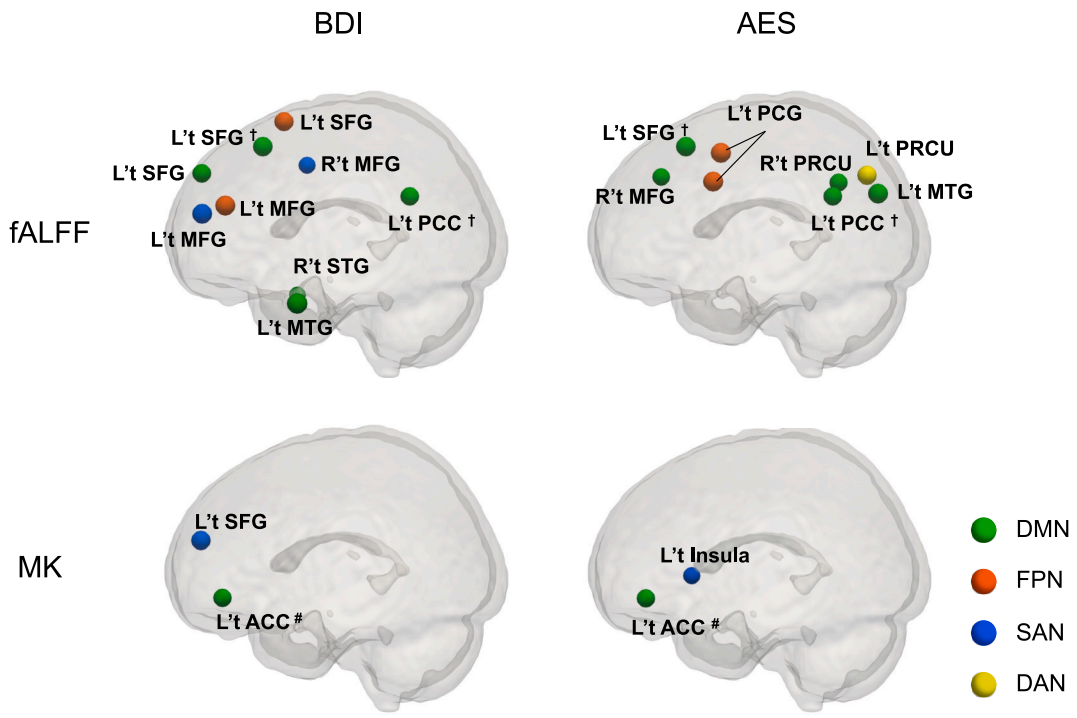

Fig. 2. Summary of hubs by depressive symptoms and apathy in dementia patients. The topological distribution of hubs contrasted by comparing high/low BDI and AES is delineated. †/# denote the shared hubs between depressive symptoms and apathy. fALFF, fractional amplitude of low-frequency fluctuation; MK, mean kurtosis; L't/R't, Left/Right; PCC, posterior cingulate cortex; SFG, superior frontal gyrus; MFG, middle frontal gyrus; STG, superior temporal gyrus; MTG, middle temporal gyrus; PRCU, precuneus; PCG, precentral gyrus; ACC, anterior cingulated cortex; SMG, supramarginal gyrus; DMN, default mode network; FPN, fronto-parietal network; SAN, salience network; DAN, dorsal attention network. See Supplementary Data Table 1-4 for detailed statistics.

3.4. Variations in neuronal correlates for depressive symptoms and apathy by dementia subtype

3.4.1. fALFF dataset

Table 3 shows the correlations between fALFF in the identified hubs and BDI/AES. After controlling for age, education, dementia subtype, and cognitive symptom duration, analysis of all participants showed that fALFF was inversely correlated with BDI in the DMN, FPN, and SAN, and inversely correlated with AES in the DMN, FPN, and DAN (all $P = 0<.001$-0.004). The left SFG within the DMN remained significantly correlated with BDI with additional control for AES, and the left PCC in the DMN, the left precentral gyrus in the FPN, and the left precuneus in the DAN remained significantly correlated with AES with additional control for BDI. Analysis of all dementia patients showed similar results, but only the left precentral gyrus was significantly correlated with AES after additional control for BDI. Of note, in contrast to the AES correlation within the DMN/DAN and BDI correlation within the DMN/SAN found in the SIVD group, no significant differences were found in the AD group, with only one FPN region at the boundary of significance in correlation with AES (left precentral gyrus; $r = -0.365$, $P = 0.012$). The linear regression analysis of all participants showed that the left SFG within the DMN to be significant hub for BDI ($\beta = -0.244$, $P = 0.004$) after controlling for age, education, cognitive symptom, and AES. The linear regression analysis showed the attenuated statistical power, with only a trend identified by the left precentral gyrus in the FPN ($\beta = -2.338$, $P = 0.021$) across AES hubs after controlling for age, education, cognitive symptoms, and BDI.

3.4.2. MK dataset

Table 4 shows correlations between MK in the identified hubs and BDI/AES. Correlation analysis of all participants, with age, education, dementia subtype, and cognitive symptom duration as covariates, showed that MK within the left ACC was inversely correlated with BDI ($P < 0.001$), and that the left ACC/right insula were inversely correlated with AES (both $P < 0.001$). The two hubs of AES correlates remained significant after additional control for BDI (indicated by ¶ in Table 4). The analysis of all dementia patients showed similar results, but only the right insula was significantly correlated with AES after additional

control for BDI. Of note, while the BDI/AES correlations in the AD group were similar to those in all dementia patients, the SIVD group only presented significance in the correlation between MK of the right insula and AES. The linear regression analysis of all participants showed that the right insula within the SAN was a significant hub for AES ($\beta = -0.285$, $P = 0.003$) after controlling for age, education, cognitive symptoms, and BDI.

4. Discussion

4.1. Shared and distinct hubs between depressive symptoms and apathy: concept, construct, and clinical implications

Our results present a paradigm showing the shared and distinct hubs of depressive symptoms and apathy using dual-modal MRI metrics. These hubs were identified by contrasting the level of depressive symptoms and apathy separately via fALFF and MK, providing a critical representation of functional and microstructural neurobiological substrates. The shared and distinct hubs were then examined by their linear associations with depressive/apathy symptoms among subgroups across the aging spectrum. There are several important findings in this study. First, compared to MK, fALFF provided a spatially broader interpretation, which corroborates the dynamic property of depressive symptoms and apathy in dementia (Supplementary Data Table 1–2 vs. 3–4). Specifically, rs-fMRI metrics are expected to show more correlations based on the known fluctuations in these two neuropsychiatric symptoms (Withall, 2011). Second, MRI metrics were correlated more consistently with apathy than with depressive symptoms in both analysis of the whole aging spectrum and dementia group (Table 3-4). This indicates the likelihood that apathy has a longer duration and more progressive nature than depressive symptoms among people with dementia. Therefore, the current findings provide a valuable reference for considering rs-fMRI and DKI metrics as surrogate biomarkers for corresponding neuropsychiatric symptoms. Third, the shared hubs can be regarded as a potential therapeutic target, while the distinct hubs may be able to assist in differential diagnostics. This is particularly important since discerning apathy from depressive symptoms at the initial assessment can be challenging, and timely interventions are needed in clinical practice. As both apathy and depressive symptoms can be a harbinger of cognitive decline (Steffens, 2022), they have both been suggested as targets for dementia treatment (Mortby, 2022; Dafsari and Jessen, 2020). Our results additionally provide a reference for tailoring therapeutic strategies according to dementia subtype.

4.2. Greater extent of apathy neurocorrelates than depressive symptoms

To date, research aimed at direct comparisons of neuroimaging substrates between apathy and depressive symptoms remains limited (Douven, 2017; Onoda and Yamaguchi, 2015; Dan, 2017). Therefore, the current dual-modal MRI protocol can extend the understanding of these two neuropsychiatric symptoms from an integrated viewpoint. The greater extent of neurocorrelates in apathy than depression has been reported with volumetric structural MRI (Lavretsky, 2008) and DTI (Hollocks, 2015; Tay, 2019). Our results also showed that apathy showed a greater extent of neurocorrelates both in the whole aging spectrum (i.e., SIVD + AD + NC) and the dementia group (i.e., SIVD + AD). These findings may be attributed to more extended operational time-frame changes (i.e., $\geq$ four weeks vs. $\geq$ two weeks) (Lanctôt, 2023) or the more progressive nature inherently observed with apathy than depression (Lanctôt, 2023). Topologically, it is worth mentioning that the fALFF hubs correlated with BDI and AES tended to be distributed within the anterior and posterior poles, respectively. The differential correlates between apathy and depressive symptoms are also compatible with previous reports using rs-fMRI across various populations (Onoda and Yamaguchi, 2015; Dan, 2017), and are in line with clinical observations, in which apathy/depressive symptoms can progress in a nonparallel manner (Withall, 2011; Connors, 2023; Yuen, 2014) and differ regarding both therapeutic response (Yuen, 2014) and prognosis (Zahodne, 2013).

Of note, our results showed that the majority of neurocorrelates in depressive/apathy symptoms were in DMN and FPN regions, which overlap considerably with the proposed limbic association tracts (Hollocks, 2015; Douven, 2017) and frontostriatal circuitry (Douven, 2017; Steffens, 2022) in the literature. The left ACC, left PCC, and left SFG appeared to be the critical hubs shared between apathy and depressive symptoms in our data, indicating that reward assessment (Rolls, 2019), action-related information processing (Rolls, 2019), and working memory (Briggs, 2020) are the potential cognitive mechanisms underpinning these two neuropsychiatric symptoms. Given the sophisticated tracts stemming from the callosal fiber bundle to the SFG (Briggs, 2020), these three hubs are related to emotion and action-outcome learning (Rolls, 2019). On the other hand, the differential microstructural/functional involvement indicated the different neurobiological nature between apathy and depressive symptoms. Specifically, functional changes within the SAN and DAN were related to depressive symptoms and apathy, respectively, whereas the microstructural changes within the DMN and DMN/SAN were primarily related to depressive symptoms and apathy, respectively. The functional aspect is in line with our previous rs-fMRI study showing significant associations between DAN and apathy construct (Altunkaya, 2022). Although it is difficult to reconcile the findings of rs-fMRI/DKI within the SAN concerning apathy and depressive symptoms at present, the significance of the SAN in apathy in late-life depression has been noted in other studies using functional (Yuen, 2014) and structural MRI (Pimontel, 2021). While the patients who suffered from apathy and depressive symptoms both showed diminished expressive motion of body and hands, our behavioral observation suggests those with high AES were prone to lose eye contact, and those with high BDI tended to avoid eye contact. Given that DAN governs voluntary eye movement to visuospatial stimuli (Kincade, 2005), it is plausible that patients with high AES scores may exhibit diminished activity within the DAN, leading to a reduced capacity for voluntary attentional control. This impairment could manifest clinically as a loss of eye contact, reflecting a deficit in sustaining attention on socially relevant stimuli. On the other hand, the associations between SAN and depressive symptoms can be extrapolated by the role of SAN in self-awareness through multi-sensory integration with mood engagement. As such, individuals with high BDI scores may experience heightened sensitivity to negative or self-referential stimuli, potentially mediated by the SAN. The depressed patients may have excessive attention allocation to self-referential thoughts or distressing social cues. One recent study also highlights the border shift and area expansion of SAN among subjects with depression (Lynch, 2024). The appetite changes have been associated with functional changes within SAN among variable cohorts (Sewaybricker, 2020; Fang, 2015). While the causality awaits to be confirmed, the mechanisms regarding SAN in appetite changes may involve reward, interoceptive neurocircuitry, and hedonic inferences of food stimuli (Cosgrove, 2020). It is also worth mentioning that the shared hubs between depressive symptoms and apathy primarily centered at the cingulate cortex and superior frontal gyrus in this cohort (Table 3 and 4). Notably, the superior frontal gyrus, together with other portions of the prefrontal cortices, has often been associated with emotion and cognition regulation (Wu et al., 2024).

4.3. Rs-fMRI showed more neurocorrelates than DKI in both depressive symptoms and apathy

Our data indicated that fALFF was more resilient than MK in exploring the neurocorrelates of depressive symptoms and apathy. Even after considering the interactions between apathy and depression, fALFF provided more robust correlations than MK. The difference in the neurophysiological property represented by these two metrics may be one of the reasons. While fALFF surrogates a composite functional

activity driven by local and remote neuronal ensembles, MK represents the local microstructural integrity. As there were more pervasive fALFF changes than MK in the current study, we underpinned the potential of fALFF to contrast the state-dependent changes among patients including variable dementia subtypes (i.e., transdiagnostic paradigm). It should be noted that the current results do not negate the strength of MK. As the regional vulnerability and pathology differs by dementia subtype, the disease subtype can cast considerable variance onto MK in a transdiagnostic paradigm. Such an effect is likely to attenuate detectable state-dependent changes in MK. As per diagnostic timeframe, apathy and depressive symptoms may develop within weeks, and the functional changes are speculated to present prior to later microstructural alterations. Concerning the dynamic nature of apathy and depressive symptoms, rs-fMRI may be a more feasible approach for investigating neuropsychiatric symptoms. In the literature, the frequency of post-stroke depression/apathy has been shown to be dependent on the stroke phase (Douven, 2017). A certain proportion of affected cases can show improvements within weeks to months, in which the cerebral function changes might be deterministic (Kennedy et al., 2015; Liu, 2023). Similarly, the prevalence of depression and apathy has also been shown to vary over time through longitudinal follow-up (Laganà, 2022). In addition to the dynamic property, a trend of an association between left-side stroke and depression/apathy formation during the acute/post-acute phase has also been reported (Douven, 2017). Several studies have also reported laterality (Tu, 2017; Kim, 2011; Tunnard, 2011). As our data also revealed left-laterality regarding depressive/apathy symptoms, our cohort could support this phenomenon. Nevertheless, knowing that laterality regarding apathy and depressive symptoms can vary by study phase (Douven, 2017; Wei, 2015) as well as study selection (Douven, 2017; Caeiro, 2013), future studies should focus on identifying determinants to disentangle such issues.

4.4. Variations in neurocorrelates of BDI/AES by dementia subtype

While our data indicated that more neurocorrelates were obtained using fALFF than MK in the whole aging spectrum, the subgroup analysis of SIVD and AD revealed the complementary value of dual-modal MRI. In particular, the hubs identified by fALFF showed more correlates in the SIVD group, while the hubs identified by MK showed more correlates in the AD group.

These findings may be associated with the differential neurosubstrates between SIVD and AD. Regarding to the more noticeable fALFF correlates in SIVD than AD, several studies have already addressed the different fMRI profiles between SIVD and AD (Altunkaya, 2022; Fu, 2019; Tu, 2020). Of note, some fMRI studies reported more noticeable functional correlates for apathy (Altunkaya, 2022) and attention (Tu, 2020) in SIVD than AD. It is known that specific pathological hallmarks of SIVD including lacunes and leukoaraiosis can damage white matter integrity and impair connections across cortices. Furthermore, altered functional connectivity has been observed among subjects burdened by SIVD pathologies during their prodromal stage (Liu, 2019; Li et al., 2012). Consequently, we speculate that a more noticeable fALFF correlates for apathy in SIVD than AD is a part of phenomenon related to the disconnection syndrome.

As for a more noticeable MK correlates in AD comparing to SIVD, the microstructural changes measured by MK have been reported among AD spectrum disorders (Song, 2019). The inversed associations between MK and BDI/AES across dementia subtypes represent that a decrease in MK was in line with compromised organizational complexity in the brain, where the compromised organizational complexity is associated with the formation of depressive symptoms and apathy. While the MK correlates within cortices are slightly more detectable in AD than in SIVD, our findings do not negate the value of DKI in detecting the microstructural changes within gray matter in any specific dementia subtype. In fact, the thalamus has been highlighted and validated to be the critical hub in SIVD, as reflected by several DKI metrics (Tu, 2021; Tu, 2024). Our results clearly delineated that the structural and functional degenerative processes were not topologically synchronized, hence emphasizing the notion of using multimodal MRI to cover the variance inherent to dementia subtypes.

Given that lower cognitive scores present with heightened AES and BDI, the negative cognitive impact was linked to apathy and depressive symptoms. The strength of this study is the utilization of dual-modal MRI techniques, comprehensive neuropsychiatric evaluations, and adequate case numbers of the two dementia subtypes. The dual-modal MRI provides the potential for diagnosing apathy/depressive symptoms among dementia and might serve as a novel biomarker for disease and therapeutics monitoring. For example, the shared hubs can provide valuable references for nonpharmacological intervention such as transcranial magnetic stimulation, and the distinct hubs may assist symptom characterization or evaluation. With advent of validated research, a more delicate protocol tailored by dementia subtypes in the future is expected to bridge dual-modal MRI to clinical use. Nevertheless, several limitations should be noted. First, we acknowledge that several items in BDI and AES may overlap. Depressive and apathy symptoms coexisted in a certain portion of the current study population (Supplementary Data Fig. 1). Therefore, we conceptualized shared and distinct hubs in our study design and reported the findings with or without BDI/AES as covariates wherever appropriate. Second, as both aging and disease effects are inherently associated with dementia, the neuronal substrates reflected by MRI metrics can be partly confounded by the aging process. However, we believe that the disease effect (i.e., dementia diagnosis and subtyping in this study) predominantly contributed to the current findings since we carefully considered age across all statistics, together with comparable age status across BDI/AES grouping in this study. Given that many other functional/microstructural imaging metrics could also be associated with variable neurobiological property, a systematic comparisons across potential metrics (e.g., ALFF, fALFF, and regional homogeneity (Deng, 2022) can be one of the research directions. Third, we did not recruit patients with intracranial hemorrhage, hence excluding potential effects driven by macroscopic hemorrhage (Douven, 2017) on apathy and/or depression formation. In addition, the recruited dementia subtypes only covered AD and SIVD. Examining patients with other dementia subtypes is warranted before concluding the shared hubs. As our cross-sectional study was constrained to observations of chronic neurodegenerative processes, the probable alterations of MRI metrics relevant to the acute phase as well as its longitudinal evolution may be explored in future studies.

5. Conclusion

Our rs-fMRI analysis revealed that both depressive symptoms and apathy involved DMN and FPN regions. Depressive symptoms and apathy were additionally involved in SAN and DAN, respectively. Our DKI analysis showed that both depressive symptoms and apathy were involved in the left ACC, while apathy was additionally involved in the right insula. Given that the functional and microstructural neurosubstrates exhibited fluidic patterns and varied by dementia subtype, we believe that dual-modal MRI metrics can provide in-depth neurobiological information underpinning depressive symptoms and apathy among dementia patients.

6. Ethics statement

This study was approved by the Research Ethics Committee of the Hospital (#REC-107–28). Written informed consent was obtained from all participants.

CRediT authorship contribution statement

Sheng-Min Huang: Writing – original draft, Visualization, Software, Methodology, Funding acquisition, Formal analysis. **Yen-Hsuan Hsu:**

Writing – review & editing, Investigation, Data curation. **Jir-Jei Yang:** Project administration, Data curation. **Chien-Yuan Lin:** Data curation. **Min-Chien Tu:** Writing – review & editing, Writing – original draft, Resources, Funding acquisition, Formal analysis, Conceptualization. **Li-Wei Kuo:** Writing – review & editing, Supervision, Resources, Project administration, Funding acquisition.

Funding

National Science and Technology Council in Taiwan, Grant/Award Numbers: NSTC-111-2221-E-400-001-MY2 (to L.W.K.), NSTC-113–2314-B-006–119 (to S.M.H.); National Health Research Institutes, Grant/Award Numbers: NHRI-BN-112-PP-06 (to L.W.K.).

2.6. Data availability

The data that support the findings of this study are available from the corresponding author upon reasonable request.

Declaration of Competing Interest

The authors declare that they have no known competing financial interests or personal relationships that could have appeared to influence the work reported in this paper.

Acknowledgement

The authors thank the patients and their caregivers for their time and commitment to this research.

Appendix A. Supplementary data

Supplementary data to this article can be found online at https://doi.org/10.1016/j.nicl.2025.103781.

Data availability

Data will be made available on request.

References

Miller, D.S., et al., 2021. *Diagnostic criteria for apathy in neurocognitive disorders.* Alzheimer's & Dementia 17 (12), 1892–1904.
Cipriani, G., et al., 2015. *Depression and dementia. A Review.* European Geriatric Medicine 6 (5), 479–486.
Chand, S.P., H. Arif, and R.M. Kutlenios, *Depression (nursing)*, in *StatPearls [Internet]*. 2023, StatPearls Publishing.
Mann, R.S., 1990. *Differential diagnosis and classification of apathy.* Am J Psychiatry 147 (1), 22–30.
Lanctôt, K.L., et al., 2023. *Distinguishing apathy from depression: A review differentiating the behavioral, neuroanatomic, and treatment-related aspects of apathy from depression in neurocognitive disorders.* International Journal of Geriatric Psychiatry 38 (2), e5882.
Benoit, M., et al., 2012. *Apathy and depression in mild Alzheimer's disease: a cross-sectional study using diagnostic criteria.* Journal of Alzheimer's Disease 31 (2), 325–334.
Mortby, M.E., et al., 2022. *Apathy as a treatment target in Alzheimer's disease: implications for clinical trials.* The American Journal of Geriatric Psychiatry 30 (2), 119–147.
Wouts, L., et al., 2020. *Empirical support for the vascular apathy hypothesis: A structured review.* International Journal of Geriatric Psychiatry 35 (1), 3–11.
Harris, M.A., et al., 2022. *Structural neuroimaging measures and lifetime depression across levels of phenotyping in UK biobank.* Translational Psychiatry 12 (1), 157.
Kempton, M.J., et al., 2011. *Structural neuroimaging studies in major depressive disorder: meta-analysis and comparison with bipolar disorder.* Archives of General Psychiatry 68 (7), 675–690.
Agüera-Ortiz, L., et al., 2017. *Structural correlates of apathy in Alzheimer's disease: a multimodal MRI study.* International Journal of Geriatric Psychiatry 32 (8), 922–930.
Zhuo, C., et al., 2019. *The rise and fall of MRI studies in major depressive disorder.* Translational Psychiatry 9 (1), 335.
Tu, M.-C., et al., 2017. *Comparison of neuropsychiatric symptoms and diffusion tensor imaging correlates among patients with subcortical ischemic vascular disease and Alzheimer's disease.* BMC Neurology 17 (1), 144.
Tu, M.C., et al., 2021. *Discriminating subcortical ischemic vascular disease and Alzheimer's disease by diffusion kurtosis imaging in segregated thalamic regions.* Human Brain Mapping 42 (7), 2018–2031.
Le Heron, C., Apps, M.A.J., Husain, M., 2018. *The anatomy of apathy: A neurocognitive framework for amotivated behaviour.* Neuropsychologia 118 (Pt B), 54–67.
Yang, H., et al., 2016. *Alterations in regional homogeneity of resting-state brain activity in patients with major depressive disorder screening positive on the 32-item hypomania checklist (HCL-32).* Journal of Affective Disorders 203, 69–76.
Tumati, S., et al., 2020. *Functional network topology associated with apathy in Alzheimer's disease.* Journal of Affective Disorders 266, 473–481.
Wise, T., et al., 2017. *Instability of default mode network connectivity in major depression: a two-sample confirmation study.* Translational Psychiatry 7 (4), e1105–e.
Altunkaya, S., et al., 2022. *Dissociable functional brain networks associated with apathy in subcortical ischemic vascular disease and Alzheimer's disease.* Frontiers in Aging Neuroscience 13, 717037.
Veer, I.M., et al., 2010. *Whole brain resting-state analysis reveals decreased functional connectivity in major depression.* Frontiers in Systems Neuroscience 4, 41.
Kim, J.W., et al., 2011. *Microstructural alteration of the anterior cingulum is associated with apathy in Alzheimer disease.* The American Journal of Geriatric Psychiatry 19 (7), 644–653.
Hollocks, M.J., et al., 2015. *Differential relationships between apathy and depression with white matter microstructural changes and functional outcomes.* Brain 138 (12), 3803–3815.
Starkstein, S.E., et al., 2009. *Neuroimaging correlates of apathy and depression in Alzheimer's disease.* The Journal of Neuropsychiatry and Clinical Neurosciences 21 (3), 259–265.
Douven, E., et al., 2017. *Imaging markers of post-stroke depression and apathy: a systematic review and meta-analysis.* Neuropsychology Review 27, 202–219.
Onoda, K., Yamaguchi, S., 2015. *Dissociative contributions of the anterior cingulate cortex to apathy and depression: topological evidence from resting-state functional MRI.* Neuropsychologia 77, 10–18.
Dan, R., et al., 2017. *Separate neural representations of depression, anxiety and apathy in Parkinson's disease.* Scientific Reports 7 (1), 12164.
Guy, M., McKhann,, et al., 2011. *The diagnosis of dementia due to Alzheimer's disease: Recommendations from the National Institute on Aging-Alzheimer's Association workgroups on diagnostic guidelines for Alzheimer's disease.* Alzheimer's & Dementia 7, 263–269.
Erkinjuntti, T., et al., 2000. *Research criteria for subcortical vascular dementia in clinical trials.* Advances in Dementia Research 23–30.
Diniz, B.S., et al., 2013. *Late-life depression and risk of vascular dementia and Alzheimer's disease: systematic review and meta-analysis of community-based cohort studies.* The British Journal of Psychiatry 202 (5), 329–335.
Jørgensen, I.F., et al., 2020. *Age-stratified longitudinal study of Alzheimer's and vascular dementia patients.* Alzheimer's & Dementia 16 (6), 908–917.
Hachinski, V.C., et al., 1975. *Cerebral blood flow in dementia.* Archives of Neurology 32 (9), 632–637.
Beck, A.T., Steer, R.A., Brown, G., 1996. *Beck depression inventory–II.* Psychological Assessment.
Hsieh, C.J., et al., 2012. *Validation of apathy evaluation scale and assessment of severity of apathy in Alzheimer's disease.* Psychiatry and Clinical Neurosciences 66 (3), 227–234.
Fuh, J.-L., et al., 2001. *Behavioral disorders and caregivers' reaction in Taiwanese patients with Alzheimer's disease.* International Psychogeriatrics 13 (1), 121–128.
Cox, R.W., 1996. *AFNI: software for analysis and visualization of functional magnetic resonance neuroimages.* Computers and Biomedical Research 29 (3), 162–173.
Tournier, J.D., et al., 2019. *MRtrix3: A fast, flexible and open software framework for medical image processing and visualisation.* Neuroimage 202, 116137.
Manjón, J.V., et al., 2013. *Diffusion weighted image denoising using overcomplete local PCA.* PloS One 8 (9).
Tabesh, A., et al., 2011. *Estimation of tensors and tensor-derived measures in diffusional kurtosis imaging.* Magn Reson Med 65 (3), 823–836.
Power, J.D., et al., 2011. *Functional network organization of the human brain.* Neuron 72 (4), 665–678.
Zou, Q.-H., et al., 2008. *An improved approach to detection of amplitude of low-frequency fluctuation (ALFF) for resting-state fMRI: fractional ALFF.* Journal of Neuroscience Methods 172 (1), 137–141.
Lakens, D., 2013. *Calculating and reporting effect sizes to facilitate cumulative science: a practical primer for t-tests and ANOVAs.* Frontiers in Psychology 4, 863.
Withall, A., et al., 2011. *A longitudinal study examining the independence of apathy and depression after stroke: the Sydney Stroke Study.* International Psychogeriatrics 23 (2), 264–273.
Steffens, D.C., et al., 2022. *The neurobiology of apathy in depression and neurocognitive impairment in older adults: a review of epidemiological, clinical, neuropsychological and biological research.* Translational Psychiatry 12 (1), 525.
Dafsari, F.S., Jessen, F., 2020. *Depression—an underrecognized target for prevention of dementia in Alzheimer's disease.* Translational Psychiatry 10 (1), 160.
Lavretsky, H., et al., 2008. *The MRI brain correlates of depressed mood, anhedonia, apathy, and anergia in older adults with and without cognitive impairment or dementia.* International Journal of Geriatric Psychiatry: A Journal of the Psychiatry of Late Life and Allied Sciences 23 (10), 1040–1050.
Tay, J., et al., *Apathy is associated with large-scale white matter network disruption in small vessel disease.* Neurology, 2019. **92**(11): p. e1157-e1167.
Connors, M.H., et al., 2023. *Distinguishing apathy and depression in dementia: A longitudinal study.* Australian & New Zealand Journal of Psychiatry 57 (6), 884–894.
Yuen, G.S., et al., 2014. *Neuroanatomical correlates of apathy in late-life depression and antidepressant treatment response.* Journal of Affective Disorders 166, 179–186.
Zahodne, L.B., et al., 2013. *Are apathy and depression independently associated with longitudinal trajectories of cortical atrophy in mild cognitive impairment?* The American Journal of Geriatric Psychiatry 21 (11), 1098–1106.

Rolls, E.T., 2019. *The cingulate cortex and limbic systems for emotion, action, and memory*. Brain Structure and Function 224 (9), 3001–3018.
Briggs, R.G., et al., 2020. *Anatomy and white matter connections of the superior frontal gyrus*. Clinical Anatomy 33 (6), 823–832.
Yuen, G.S., et al., 2014. *The salience network in the apathy of late-life depression*. International Journal of Geriatric Psychiatry 29 (11), 1116–1124.
Pimontel, M.A., et al., 2021. *Cortical thickness of the salience network and change in apathy following antidepressant treatment for late-life depression*. The American Journal of Geriatric Psychiatry 29 (3), 241–248.
Kincade, J.M., et al., 2005. *An event-related functional magnetic resonance imaging study of voluntary and stimulus-driven orienting of attention*. Journal of Neuroscience 25 (18), 4593–4604.
Lynch, C.J., et al., 2024. *Frontostriatal salience network expansion in individuals in depression*. Nature 633 (8030), 624–633.
Sewaybricker, L.E., et al., 2020. *Salience network connectivity is reduced by a meal and influenced by genetic background and hypothalamic gliosis*. International Journal of Obesity 44 (1), 167–177.
Fang, Z., et al., 2015. *Altered salience network connectivity predicts macronutrient intake after sleep deprivation*. Scientific Reports 5 (1), 8215.
Cosgrove, K.T., et al., 2020. *Appetite change profiles in depression exhibit differential relationships between systemic inflammation and activity in reward and interoceptive neurocircuitry*. Brain, Behavior, and Immunity 83, 163–171.
Wu, D., J. Li, and J. Wang, *Altered neural activities during emotion regulation in depression: a meta-analysis.* Journal of Psychiatry and Neuroscience, 2024. **49**(5): p. E334-E344.
Kennedy, J.M., Granato, D.A., Goldfine, A.M., 2015. *Natural history of poststroke apathy during acute rehabilitation*. The Journal of Neuropsychiatry and Clinical Neurosciences 27 (4), 333–338.
Liu, L., et al., 2023. *Prevalence and natural history of depression after stroke: A systematic review and meta-analysis of observational studies*. PLoS Medicine 20 (3), e1004200.
Laganà, V., et al., 2022. *Neuropsychiatric or Behavioral and Psychological Symptoms of Dementia (BPSD): focus on prevalence and natural history in Alzheimer's Disease and Frontotemporal Dementia*. Frontiers in Neurology 13, 832199.
Tunnard, C., et al., 2011. *Apathy and cortical atrophy in Alzheimer's disease*. International Journal of Geriatric Psychiatry 26 (7), 741–748.
Wei, N., et al., 2015. *Post-stroke depression and lesion location: a systematic review*. Journal of Neurology 262, 81–90.
Caeiro, L., et al., 2013. *Post-stroke apathy: an exploratory longitudinal study*. Cerebrovascular Diseases 35 (6), 507–513.
Fu, Z., et al., 2019. *Altered static and dynamic functional network connectivity in Alzheimer's disease and subcortical ischemic vascular disease: shared and specific brain connectivity abnormalities*. Human Brain Mapping 40 (11), 3203–3221.
Tu, M.-C., et al., 2020. *Attention and functional connectivity among patients with early-stage subcortical ischemic vascular disease and Alzheimer's disease*. Frontiers in Aging Neuroscience 12.
Liu, X., et al., 2019. *Altered functional connectivity in patients with subcortical ischemic vascular disease: a resting-state fMRI study*. Brain Research 1715, 126–133.
Li, C., Zheng, J., Wang, J., 2012. *An fMRI study of prefrontal cortical function in subcortical ischemic vascular cognitive impairment*. American Journal of Alzheimer's Disease & Other Dementias® 27 (7), 490–495.
Song, G.-P., et al., 2019. *Differentiating between Alzheimer's disease, amnestic mild cognitive impairment, and normal aging via diffusion kurtosis imaging*. Neural Regeneration Research 14 (12), 2141.
Tu, M.-C., et al., 2024. *Joint diffusional kurtosis magnetic resonance imaging analysis of white matter and the thalamus to identify subcortical ischemic vascular disease*. Scientific Reports 14 (1), 2570.
Deng, S., et al., 2022. *Hemodynamic and metabolic correspondence of resting-state voxel-based physiological metrics in healthy adults*. Neuroimage 250, 118923.
Yan, C.-G., Zang, Y.-F., 2010. *DPARSF: A MATLAB Toolbox for "Pipeline" Data Analysis of Resting-State fMRI*. Front Syst Neurosci 4, 13.